OPEN

NPG Asia Materials (2017) 9, e374; doi:10.1038/am.2017.48
www.nature.com/am

ORIGINAL ARTICLE

New photopatternable polyimide and programmable nonvolatile memory performances

Suk Gyu Hahm, Samdae Park and Moonhor Ree

We report the first photopatternable, nonvolatile memory consisting of high-temperature polyimide (PI), poly (hexafluoroisopropylidenediphthalimide-4-cinnamoyloxytri-phenylamine) (6F-HTPA-CI), and we demonstrate the successful fabrication and programmable operation of 'write-read-erase' memory devices based on nanoscale thin films of 6F-HTPA-CI. The PI thin film enables scalable fine patternability, providing lines and spaces with excellent pattern fidelity. Isolated individual memory devices were successfully fabricated on a bottom electrode via a sequential process of coating, photopatterning, top electrode deposition, developing, rinsing and drying. The 6F-HTPA-CI cells exhibited excellent nonvolatile memory performances in three different modes (unipolar permanent, unipolar flash and bipolar flash memories), regardless of photo-exposure doses. The switching-ON (writing) voltage was in the range of ± 1.5 to ± 2.0 V, and the switching-OFF (erasing) voltage was in the range of ± 0.3 to ± 0.8 V; these voltages are quite low, indicating that power consumption by the devices during operation is low. The ON/OFF current ratio of the devices was in the range of 10^4–10^9. Overall, the photopatternable PI 6F-HTPA-CI opens up the possibility of low-cost mass production of high-performance, high-speed, energy-efficient, permanent or rewritable high-density nonvolatile polymer memory devices suitable for future advanced electronics in highly integrated systems.
NPG Asia Materials (2017) **9,** e374; doi:10.1038/am.2017.48; published online 14 April 2017

INTRODUCTION

Electrically nonvolatile memory materials have recently attracted considerable attention because of their broad applicability in future microelectronic devices such as flexible displays, electronic skin, radio-frequency identification or near-field communication tags and wearable stretchable sensors into which memory devices are incorporated.[1–5] The integration of memory chips with logic chips, displays and sensors in a single, flexible platform is one of the most important challenges for the realization of future microelectronics.[4,5] Resistive random access memory produced from silicon- or metal-oxide-based materials is an emerging class of high-performance nonvolatile memory.[6,7] However, these memory materials are mechanically incompatible with flexible, bendable or stretchable substrates because of their stiff and brittle nature.

Organic small-molecule-based nonvolatile memory materials have been proposed as alternative candidates for flexible data-storage devices.[8–13] However, this approach has been found to have restrictions such as insufficient mechanical stretchability due to the weak and brittle nature of the material and poor interfacial adhesion, long process times, low-cost efficiency due to high-temperature evaporation in vacuum and limited area deposition, and material degradation.[8–13]

By contrast, polymeric memory materials offer significant advantages, such as superb processability and excellent printability over large areas, enabling the cost-effective mass production of electronics. Moreover, their superior flexibility, toughness, dimensional stability and device properties can be easily tuned by tailoring their chemical structures during synthesis.[14–31] However, the realization of high-density polymeric memory devices in a low-cost manner is highly constrained by the fact that the majority of reported polymeric memory materials will readily degrade or dissolve upon exposure to the solvents or wet chemicals used in multilayer device fabrication processes.[21–25] Although some of these materials have high dimensional and mechanical stability, their film forms are not sufficiently resilient to survive the device fabrication process.[31–33] Furthermore, they all lack patternability and thus can be patterned only with the aid of photoresist-based lithography techniques, significantly increasing the number of steps and the cost of device fabrication. Therefore, there is still an urgent need for low-cost printable, patternable, multi-stackable memory materials that are suitable for the fabrication of high-density memory devices and further integration with other electronic devices of various functionalities.

In this study, our aim was the molecular design and synthesis of a novel digital memory polymer that can exhibit multiple functionalities, such as solution processability, patternability, post-insolubility (that is, becoming insoluble after patterning process), the capability of multilayer stacking, dimensional stability, thermal stability and electrically nonvolatile memory performance, which are

Department of Chemistry, Division of Advanced Materials Science, Pohang Accelerator Laboratory, Polymer Research Institute and BK School of Molecular Science, Pohang University of Science & Technology (POSTECH), Pohang, Republic of Korea
Correspondence: Professor M Ree, Department of Chemistry, Division of Advanced Materials Science, Pohang Accelerator Laboratory, Polymer Research Institute and BK School of Molecular Science, Pohang University of Science & Technology (POSTECH), San 31, Hyoja-dong, Nam-gu, Pohang 37673, Republic of Korea.
E-mail: ree@postech.edu
Received 28 September 2016; revised 23 January 2017; accepted 30 January 2017

required for the production of high-density and high-performance memory devices. At the molecular design stage, a soluble, high-temperature polyimide (PI) was considered as the polymer backbone because it can provide solution processability, dimensional stability and thermal stability.[16,17,33,34] A photocrosslinkable functionality was also considered. Such a functionality can provide both large-area printability and photopatternability as a noncontact, negative-tone lithography tool. This functionality can further lead to highly enhanced dimensional, chemical and thermal stabilities as well as mechanical strength by means of photocrosslink formation through the photopatterning process. This functionality can also provide a multilayer stacking capability via the photopatterning process and photoreaction-induced insolubilization. Moreover, this functionality can offer another great benefit, namely, the formation of isolated rather than interconnected memory cells from neighboring ones by means of fine patterning, enabling a significant reduction in crosstalk and current leakage, which is crucial for high-speed devices with low-energy consumption. For materials with such photocrosslinkable functionalities, there are several options, such as acryl, methacryl, cinnamoyl, stilbenyl and coumarinyl.[35–44] Finally, electrical memory function was considered. For the incorporation of electrical memory function, several candidate functional groups exist, including carbazolyl, aminotriphenyl, anthracenyl, fluorenyl, fullerenyl and aliphatic π-conjugations.[14–18]

As a result of the molecular design and synthesis effort described above, we here introduce a new photopatternable, digital-memory-programmable, high-temperature PI, poly(hexafluoroisopropylidene-diphthalimide-4-cinnamoyloxytriphenylamine) (6F-HTPA-CI), and we demonstrate the successful fabrication and programmable operation of 'write-read-erase' memory devices based on nanoscale thin films of 6F-HTPA-CI. These PI thin films exhibit scalable fine patternability, providing lines and spaces with excellent pattern fidelity. Isolated individual memory devices were successfully fabricated on a bottom electrode via a sequential process of coating, photopatterning, top electrode deposition, developing, rinsing and drying. The 6F-HTPA-CI cells exhibited excellent nonvolatile memory performances in three different modes (unipolar permanent memory, unipolar flash memory and bipolar flash memory), regardless of photo-exposure doses. The switching-ON (writing) voltage was in the range of ± 1.5 to ± 2.0 V, and the switching-OFF (erasing) voltage was in the range of ± 0.3 to ± 0.8 V; these voltages are quite low, indicating that power consumption by the devices during operation is low. The ON/OFF current ratio of the devices was in the range of $10^4 - 10^9$. Overall, the photopatternable PI 6F-HTPA-CI opens up the possibility of low-cost mass production of high-performance, high-speed, energy-efficient, permanent or rewritable high-density nonvolatile polymer memory devices suitable for future advanced electronics in highly integrated systems.

MATERIALS AND METHODS

All chemical compounds were purchased from Aldrich (St Louis, MO, USA) and used as received unless stated otherwise. The 6F-HTPA-CI was synthesized in dimethylacetamide as described in the Supplementary Scheme S1 and Supplementary Figure S1. For the polymer synthesized in dimethylacetamide with a concentration of 0.10 g dl^{-1}, the inherent viscosity was measured at 25 °C using an Ubbelohde suspended-level capillary viscometer (LK Lab Korea, South Yangju, South Korea). The polymer was characterized using an ultraviolet (UV)–visible absorption spectrometer, a thermogravimeter, a differential scanning calorimeter and an electrochemical workstation (Supplementary Information). For the fabrication of polymer memory devices, a homogeneous PI solution (1.0 wt%) was prepared in cyclopentanone and then filtered using polytetrafluoroethylene-membrane-based micro-filters with a pore size of 0.45 μm. Al/6F-HTPA-CI (unexposed or exposed to UV light)/Al devices were fabricated via the following process. First, 300 nm-thick aluminum layers were evaporated onto precleaned bare silicon wafers serving as bottom electrodes. The filtered PI solution was spin-coated onto the bottom electrodes. Then, the films were dried for 12 h in a vacuum oven at 100 °C and cooled to room temperature. The thicknesses of the obtained PI films were measured using a spectroscopic ellipsometer (model M2000, Woollam, Lincoln, NE, USA). Subsequently, the polymer films were exposed to UV light from a high-pressure Hg lamp to form patterns using shadow masks. Finally, an Al top electrode (300 nm) was deposited on top of each PI film layer via thermal evaporation with shadow masks in vacuum (10^{-6} torr). $I-V$ measurements were conducted using a Keithley 4200 semiconductor analyzer (Cleveland, OH, USA) with a maximum current compliance of 0.105 A. All experiments were performed at room temperature in ambient air.

RESULTS AND DISCUSSION

Polymer synthesis and photopatterning

6F-HTPA-CI was successfully synthesized in a four-step manner, as shown in Supplementary Scheme S1; the details of the synthesis are given along with the chemical characterization data (Supplementary Figure S1) in Supplementary Information. The 6F-HTPA-CI PI was measured to have an inherent viscosity of 0.78 dl g^{-1} at 25 °C; a PI solution of 0.10 g dl^{-1} in dimethylacetamide was used for the viscosity measurement. The glass transition temperature, T_g, was 261 °C, and the degradation temperature, T_d, was 365 °C (Supplementary Figure S2). No melting transition was observed below T_d. These results collectively confirmed that the synthesized PI polymer was a dimensionally stable, amorphous polymer below 261 °C. The PI polymer was soluble in common solvents such as cyclopentanone, dimethyl sulfoxide, *N*-methyl-2-pyrrolidone and dimethylacetamide, producing high-quality thin films (with a surface roughness of $0.1 - 0.6$ nm, depending on the substrate) via conventional solution-coating processes.

In film form (60.4 nm thick), the PI polymer exhibited an absorption maximum at a wavelength of 283 nm ($=\lambda_{max}$) in UV–visible spectroscopy, which was attributed to the CI chromophore moieties in the polymer (Supplementary Figure S3). This absorption peak drastically changed in intensity under exposure to UV light (260–380 nm). The absorption peak intensity abruptly decreased in the early stages of photo-exposure and then decreased more slowly with increasing exposure energy up to 3.0 J cm^{-2}. Thereafter, the absorption intensity level remained constant as the exposure dose was further increased to 9.0 J cm^{-2}. These results collectively indicated that the CI moieties of the PI polymer in the film underwent a favorable photocrosslinking reaction (Figure 1a).

Figure 1b shows a representative contrast curve of 6F-HTPA-CI in film form. During the lithographic process, the remaining film thickness was 40% for films exposed to UV at 0.5 J cm^{-2}, 67% for films exposed to UV at 2.0 J cm^{-2} and 83% for films exposed to UV at 5.0 J cm^{-2} or higher (up to 9.0 J cm^{-2}); the initial film thickness was 60 nm. In addition, lines (1 μm spaces and widths) and dots (25 μm in radius) were successfully patterned via the lithographic process with the aid of UV exposure and patterned masks, as shown in the insets of Figure 1b. These results collectively confirmed that the CI moieties of the developed PI polymer undergo a favorable photocrosslinking reaction and then insolubilize the UV-exposed regions of the film, demonstrating excellent photopatternability (that is, negative-tone photopatternability).

Polymer memory characteristics

For memory device fabrication, we used shadow masks with open circular dots (with diameters ranging from 50 to 100 μm) or

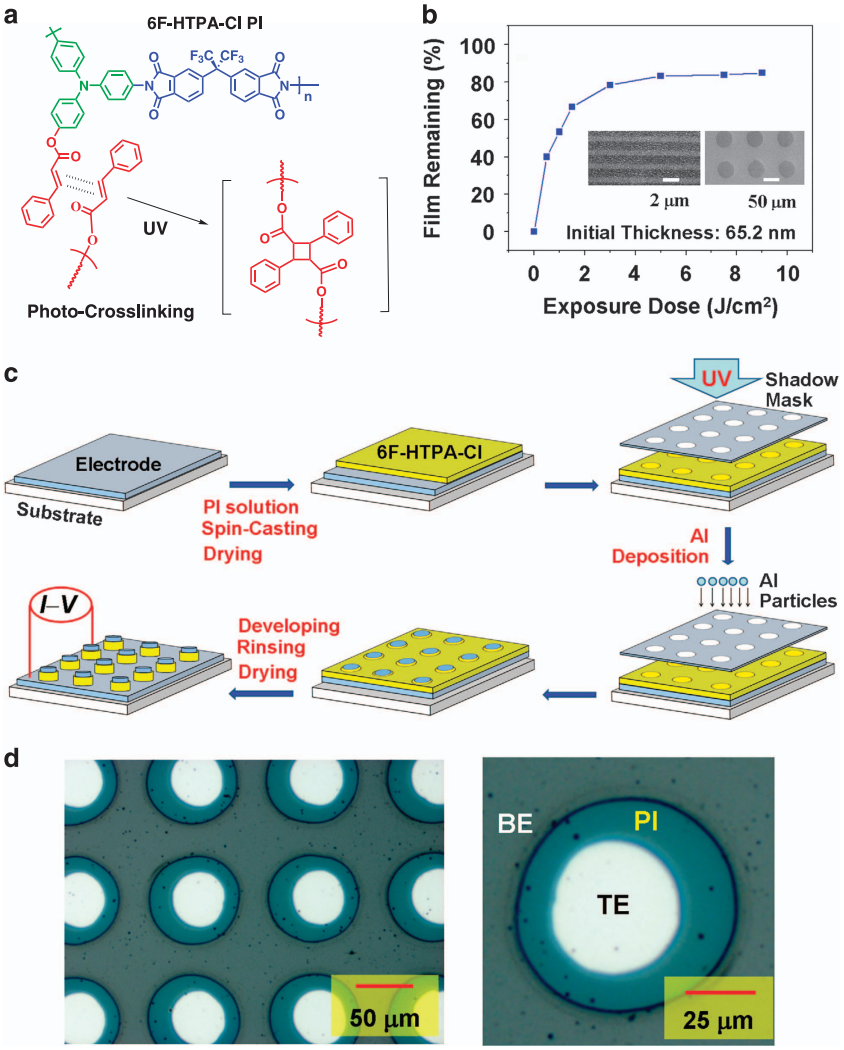

Figure 1 6F-HTPA-CI PI. (**a**) Chemical structure and photoreaction scheme of 6F-HTPA-CI in thin films. (**b**) photolithographic contrast curve of 6F-HTPA-CI films (inset: scanning electron microscopy images of patterned PI films: (left) top view of a line pattern with 1 μm line widths and spaces; (right) top view of a dot pattern with a 50 μm dot diameter). (**c**) Schematic illustration of the memory device fabrication process employed in this study. (**d**) optical microscopy images of patterned 6F-HTPA-CI PI memory device cells that were fabricated via the sequential process depicted in **c** ((left) top view of the cells; (right) memory cell under magnification). 6F-HTPA-CI, poly(hexafluoroisopropylidenediphthalimide-4-cinnamoyloxytri-phenylamine) (6F-HTPA-CI); PI, polyimide.

open rectangular dots (with areas ranging from $100 \times 100\ \mu m^2$ to $500 \times 500\ \mu m^2$). The thin 6F-HTPA-CI films were sandwiched as active layers between top and bottom electrodes via a sequential process of PI solution coating, UV exposure, metal deposition, developing with cyclopentanone, rinsing with isopropyl alcohol and drying under blowing nitrogen gas (Figure 1c). Optical microscopy images of the patterned PI memory devices with a top electrode of 50 μm in diameter are displayed in Figure 1d.

The as-fabricated PI film initially exhibited a high-resistance state (that is, an OFF state), as shown in Figure 2a. When a negative voltage was applied with a compliance current of 0.01 A, the PI film underwent a sharp electrical transition from the OFF state into the ON state at approximately −1.52 V ($=V_{c,ON}$, switching-ON voltage). This ON state was preserved even after the power was turned off or during a forward voltage sweep at the same compliance current level (0.01 A). These results collectively demonstrated that the as-fabricated PI film exhibited write-once read-many-times memory behavior (that is, a characteristic of permanent memory). When a negative voltage was again applied with the compliance current increased to 0.1 A (higher than that in the first voltage sweep), however, the PI film underwent a sharp electrical transition from the ON state to the OFF state at approximately −0.40 V ($=V_{c,OFF}$, switching-OFF voltage). Consequently, the PI film further exhibited the ability to be operated in a flash memory mode by changing the compliance current. The ON/OFF current ratio of the PI film devices was in the range of $10^5 - 10^8$, depending on the level of the turn-on compliance current and the reading voltage. Similar ON- and OFF-switching behaviors were observed in a positive voltage sweep (Figure 2b). Overall, the as-fabricated PI films demonstrated unipolar switching behaviors in two different modes, namely, nonvolatile flash and permanent memory modes, with and without changes in the compliance current settings, respectively.

PI films that were photo-exposed at 0.5 J cm^{-2} exhibited unipolar switching behaviors in dual modes (Figure 2c and d), similar to those observed for the as-fabricated PI films. The switching-ON voltage was approximately −1.47 V in the first negative voltage sweep with a 0.01 A compliance current and +1.30 V in the first positive voltage sweep. The switching-OFF voltage was −0.65 V or +0.65 V in

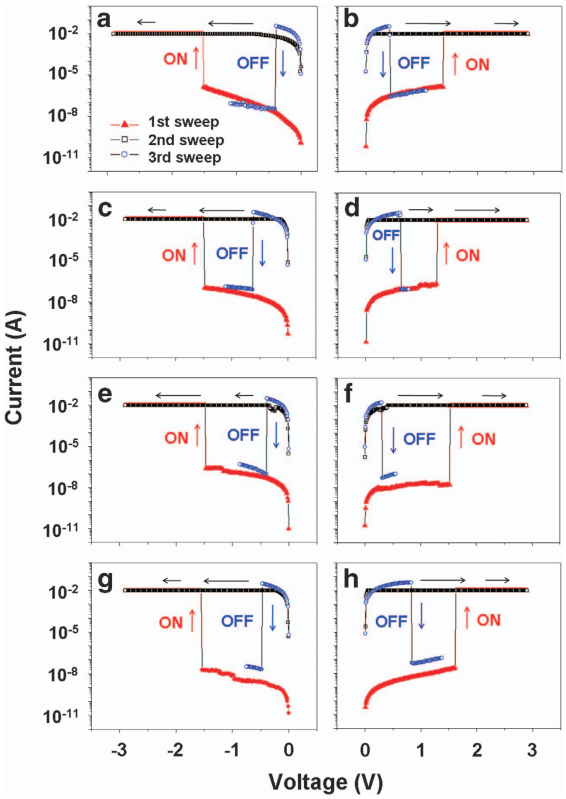

Figure 2 Unipolar *I–V* characteristics of Al/6F-HTPA-CI (61.3 – 65.2 nm thick)/Al devices. (**a**, **b**) As-fabricated PI film. (**c**, **d**) PI film exposed to UV at 0.5 J cm^{-2}. (**e**, **f**) PI film exposed to UV at 1.5 J cm^{-2}. (**g**, **h**) PI film exposed to UV at 5.0 J cm^{-2}. The sizes of the cells ranged from 100 × 100 to 500 × 500 μm^2. 6F-HTPA-CI, poly(hexafluoroisopropylidenediphthalimide-4-cinnamoyloxytri-phenylamine) (6F-HTPA-CI); UV, ultraviolet.

a voltage sweep at 0.1 A. The ON/OFF current ratio of the devices was in the range of $10^5 - 10^9$. Similar switching behaviors were demonstrated by PI films photo-exposed at higher energy doses (1.5 and 5.0 J cm^{-2}), as shown in Figure 2e–h. The results collectively confirmed that the nonvolatile memory characteristics of the PI films were not influenced by the UV exposure (that is, UV-induced crosslinking reactions) associated with the photolithographic patterning process.

Interestingly, the 6F-HTPA-CI films further exhibited bipolar characteristics. As shown in Figure 3a, the ON state that was achieved in a first negative voltage sweep at a compliance current of 0.01 A could be switched to the OFF state by a positive voltage sweep at a compliance current higher than that used in the first sweep. Similarly, the ON state generated in a first positive voltage sweep could be turned off by a negative voltage sweep at a compliance current higher than that used in the first sweep (Figure 3b).

We investigated these devices' ability to write, read and erase data, which is required in nonvolatile memory devices. Figure 4a shows the variations in $V_{c,ON}$, $V_{c,OFF}$ and the turn-OFF current for a 6F-HTPA-CI film that was UV-exposed at 5.0 J cm^{-2} during voltage sweep cycles. As the $V_{c,ON}$ value varied in the range of +1.57 to +1.92 V and the $V_{c,OFF}$ value varied in the range of +0.37 to +0.58 V, depending on the number of voltage sweep cycles, the turn-OFF current varied over the range of 0.032–0.039 A; these values are much lower than the compliance current (0.1 A) required for the switch-OFF process but slightly higher than that (0.01 A) required for the switch-ON process in the first voltage sweep. Overall, the

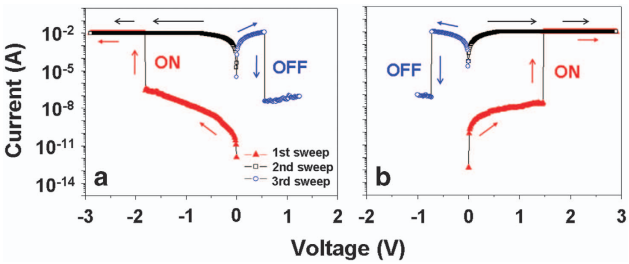

Figure 3 Bipolar *I–V* characteristics of Al/6F-HTPA-CI (61.3 nm thick, UV-exposed at 5.0 J cm^{-2})/Al devices. The first and second voltage sweeps were performed with a compliance current of 0.01 A, whereas the third sweep was performed with a compliance current of 0.1 A. 6F-HTPA-CI, poly(hexafluoroisopropylidenediphthalimide-4-cinnamoyloxytriphenylamine) (6F-HTPA-CI); UV, ultraviolet.

variations in $V_{c,ON}$ were larger than those in $V_{c,OFF}$. These results can be understood as follows. During the switch-ON process (that is, the writing or 'Set' process; Figure 2), a constant compliance current of 0.01 A is required, which could limit variations in the resistance of the ON state and further lead to small variations in $V_{c,OFF}$. By contrast, during the turn-OFF process (that is, the erasing or 'Reset' process), more random disruption of the conducting paths occurs, which could cause some variations in the resistance of the OFF state and somewhat larger variations in $V_{c,ON}$.

To investigate the influence of the turn-ON compliance current on the turn-OFF current, we further tested the 6F-HTPA-CI films by changing the turn-ON compliance current at regular intervals. As the turn-ON compliance current increased, the current required to switch off the device was found to increase (Figure 4b). In addition, as the turn-ON compliance current increased, the resistance of the ON state decreased. However, both the $V_{c,ON}$ level and the $V_{c,OFF}$ level showed relatively little variation with the changing turn-ON compliance current (Figure 4a). These results can be understood as follows. As the turn-ON compliance current is increased, more carriers become trapped near the electrode before the transition between the OFF and ON states occurs. These trapped carriers result in an increase in the number of conducting pathways and in the turn-OFF current. Accordingly, when the turn-ON compliance current is fixed, the turn-OFF current is likely to remain constant. To confirm this, the reliabilities of the turn-ON and turn-OFF voltages and the turn-OFF current were tested at a fixed turn-ON compliance current (0.01 A) by repeating the switching process. These tests confirmed that the turn-ON and turn-OFF voltages as well as the turn-OFF current remained almost constant when a positive bias was applied (Figure 4a). Similar switching behaviors were observed under the application of a negative bias (data not shown). This reliable current-controlled electrical switching behavior of the PI film memory devices can be understood by considering charge-trapping and hopping process driven by the electroactive HTPA moieties in the film: the HTPA moieties can act as charge-trapping sites as well as stepping stones for the charge-hopping process.

Figure 5 presents representative results of electrical stability (that is, retention) tests that were conducted in ambient air by alternately applying a reading voltage of +0.8 V and 0.0 V for a pulse duration of 5 ms. Once the device was switched into the ON state by applying a voltage of 2.0 V with a compliance current of 0.01 A, the ON state was retained without any degradation for the test period of 1.0×10^4 s. Moreover, it was confirmed that the device could maintain such an ON state for four months to one year. When the ON state was switched back to the OFF state by applying a voltage of 1.0 V

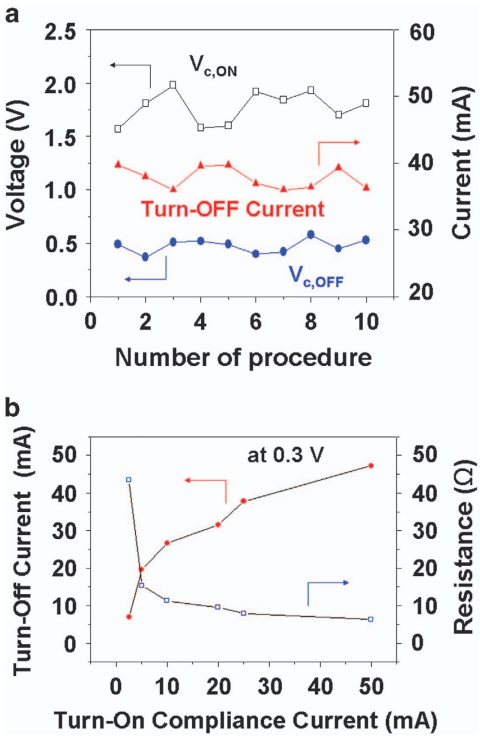

Figure 4 Al/6F-HTPA-CI (61.3 nm thick, UV-exposed at 5.0 J cm^{-2})/Al devices. (**a**) variations in $V_{c,ON}$ (turn-ON voltage), $V_{c,OFF}$ (turn-OFF voltage) and turn-OFF current during voltage sweep cycles, where in every cycle, the first sweep was performed with a compliance current of 0.01 A from 0 to +2.9 V to switch on the device, the second sweep was performed with the same compliance current from 0 to +2.9 V to maintain the ON state of the device, and the third sweep performed with a compliance current of 0.1 A to switch off the device from its ON state. (**b**) Turn-off current and resistance variations with a changing turn-ON compliance current. 6F-HTPA-CI, poly(hexafluoroisopropylidenediphthalimide-4-cinnamoyloxytri-phenylamine) (6F-HTPA-CI); UV, ultraviolet.

with a compliance current of 0.1 A, the OFF state was also found to be well retained without any degradation over the entire test period and even for 4 months to 1 year. Overall, the devices exhibited excellent reliability even in ambient air.

The highest occupied molecular orbital (E_{HOMO}) and lowest unoccupied molecular orbital (E_{LUMO}) of the PI film were determined to be −5.69 and −2.25 V, respectively, via cyclic voltammetry (Supplementary Figure S4). In an Al/6F-HTPA-CI/Al device, the energy barrier for hole injection from the electrode to the active PI layer was estimated to be 1.47 eV from the work function (Φ) of Al (−4.20 eV) and the E_{HOMO} of the active layer; the energy barrier for electron injection from the electrode to the active layer was estimated to be 1.95 eV from the Φ of Al and the E_{LUMO} of the active layer. These results indicate that the conduction process in the device is dominated by hole injection.

To understand the electrical switching characteristics of the PI devices, the measured $I-V$ data were further analyzed in detail using various conduction models.[45–49] The $I-V$ data for the OFF state could be satisfactorily fitted with a trap-limited space-charge-limited conduction model, whereas those for the ON state could be well fitted with an ohmic conduction model (Supplementary Figure S5). Further information about the charge transport mechanisms were obtained from temperature-dependent measurements (Supplementary Figure S6). The OFF-state currents that were measured for varying

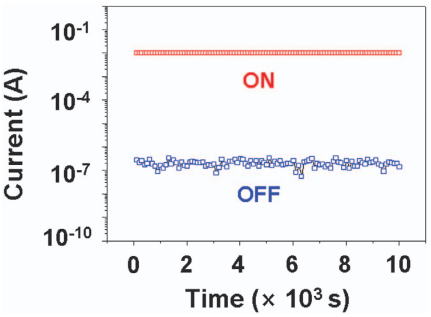

Figure 5 Long-term (that is, retention time) responses of the ON and OFF states of Al/6F-HTPA-CI (61.3 nm thick, UV-exposed at 5.0 J cm^{-2})/Al devices probed by alternately applying a reading voltage of +0.8 and 0.0 V for a pulse duration of 5 ms. The ON state ('write') was induced using a turn-ON compliance current of 0.01 A by applying a voltage of +2.0 V, whereas the OFF state ('erase') was reinstated by applying a voltage of 1.0 V with a turn-OFF compliance current of 0.1 A. 6F-HTPA-CI, poly(hexafluoroisopropylidenediphthalimide-4-cinnamoyloxytri-phenylamine) (6F-HTPA-CI); UV, ultraviolet.

temperatures at a given voltage were found to be well fitted by a thermally activated transport model with an activation energy (E_a) of 1.51 eV (Supplementary Figure S7); the ON-state currents exhibited slightly metallic behavior.[49]

The above results collectively suggested that the excellent nonvolatile memory behaviors of the PI films are governed by trap-limited space-charge-limited conduction and hopping processes. In terms of its chemical composition, the PI chain is composed of an oxytriphenylamine unit (electron donor, that is, hole transporter), a cinnamoyl end group (electron acceptor), two trifluoromethyl groups (electron acceptors) and two imide ring units (electron acceptors) per repeat unit. These units and groups may act as charge-trapping sites because of their inductive nature. However, their role and capacity as charge-trapping sites may be highly dependent upon strong support from any possible resonance effect. Considering the hole-injection-driven nature of the conduction process and the possible aid of a resonance effect, the oxytriphenylamine moieties among the chemical units and groups could play a key role in the observed nonvolatile memory behaviors. When an increasing voltage bias is applied, charges could become trapped in the trap sites until the sites' full capacity is filled (that is, very close to $V_{c,ON}$), and above $V_{c,ON}$, charges could become able to move through the trap sites (which would serve as stepping stones) by means of a hopping process, resulting in a current flow between the bottom and top electrodes under a given compliance current. When the compliance current is set at a higher level (for example, 0.1 A) than the initial turn-ON compliance current (0.01 A), a greater number of charges can flow through the previously charge-trapping sites that are serving as paths through the hopping process. Such excessive charge injection and current flow may produce heat at the charge-trapping sites and further induce repulsive Coulomb interactions between the locally trapped charges, leading to disruption of the hopping paths that had previously formed under the voltage sweep at a lower compliance current and ultimately returning the device to the OFF state.

CONCLUSION

6F-HTPA-CI exhibits facile solution processability and excellent photopatternability, producing high-quality nanoscale thin films and high-performance electrical memory cells. Our photopatterned

6F-HTPA-CI cells demonstrated three different modes of nonvolatile memory behavior: (i) unipolar write-once read-many-times memory, (ii) unipolar flash memory and (iii) bipolar flash memory. All devices could be operated at a very low power, with a voltage of less than ± 2.0 V; the ON/OFF current ratio was in the range of $10^4 - 10^9$ depending on the levels of the turn-ON compliance current and the reading voltage. The cells further exhibited excellent reliability even in ambient air. Overall, the photopatternable PI 6F-HTPA-CI is very suitable for future energy-efficient, high-speed and high-density nonvolatile memory devices.

CONFLICT OF INTEREST

The authors declare no conflict of interest.

ACKNOWLEDGEMENTS

This study was supported by the National Research Foundation (NRF) of Korea (Doyak Program 2011-0028678) and by the Ministry of Science, ICT & Future Planning (MSIP) and the Ministry of Education (BK21 Plus Program and Global Excel Program) of the Republic of Korea.

Author contributions: MR designed the research and initiated the study. SGH and SP synthesized and characterized the materials. SGH prepared the nanoscale thin films and characterized them in detail. SGH performed the device fabrication and $I-V$ analysis. MR, SGH, and SP prepared the manuscript. All authors contributed to the discussion.

1 Ouyang, J. Y., Chu, C. W., Szmanda, C. R., Ma, L. P. & Yang, Y. Programmable polymer thin film and non-volatile memory device. *Nat. Mater.* **3**, 918–922 (2004).
2 Moller, S., Perlov, C., Jackson, W., Taussig, C. & Forrest, S. R. A polymer/semiconductor write-once read-many-times memory. *Nature* **426**, 166–169 (2003).
3 Son, D., Lee, J., Qiao, S., Ghaffari, R., Kim, J., Lee, J. E., Song, C., Kim, S. J., Lee, D. J., Jun, S. W., Yang, S., Park, M., Shin, J., Do, K., Lee, M., Kang, K., Hwang, C. S., Lu, N., Hyeon, T. & Kim, D.-H. Multifunctional wearable devices for diagnosis and therapy of movement disorders. *Nat. Nanotechnol.* **9**, 397–404 (2014).
4 ThinFilm homepage, World's first printed ferroelectric memory device. Available at http://www.thinfilm.no.
5 Abad, E., Zampolli, S., Marco, S., Scorzoni, A., Mazzolai, B., Juarros, A., Gomez, D., Elmi, I., Cardinali, G. C., Gomez, J. M., Palacio, F., Cicioni, M., Mondini, A., Becker, T. & Sayhan, I. Flexible tag microlab development: Gas sensors integration in RFID flexible tags for food logistic. *Sens. Actuators B Chem.* **127**, 2–7 (2007).
6 Waser, R. & Aono, M. Nanoionics-based resistive switching memories. *Nat. Mater.* **6**, 833–840 (2007).
7 Kwon, D.-H., Kim, K. M., Jang, J. H., Jeon, J. M., Lee, M. H., Kim, G. H., Li, X.-S., Park, G.-S., Lee, B., Han, S., Kim, M. & Hwang, C. S. Atomic structure of conducting nanofilaments in TiO2 resistive switching memory. *Nat. Nanotechnol.* **5**, 148–153 (2010).
8 Aviram, A., Joachim, C. & Pomerantz, M. Evidence of switching and rectification by a single molecule effected with a scanning tunneling microscope. *Chem. Phys. Lett.* **146**, 490–495 (1988).
9 Gao, H. J., Sohlberg, K., Xue, Z. Q., Chen, H. Y., Hou, S. M., Ma, L. P., Fang, X. W., Pang, S. J. & Pennycook, S. J. Reversible, nanometer-scale conductance transitions in an organic complex. *Phys. Rev. Lett.* **84**, 1780–1783 (2000).
10 Donhauser, Z. J., Mantooth, B. A., Kelly, K. F., Bumm, L. A., Monnell, J. D., Stapleton, J. J., Price, D. W. Jr., Rawlett, A. M., Allara, D. L., Tour, J. M. & Weiss, P. S. Conductance switching in single molecules through conformational changes. *Science* **292**, 2303–2307 (2001).
11 Chen, J. & Ma, D. Single-layer organic memory devices based on N,N'-di(naphthalene-l-yl)-N,N'-diphenyl-benzidine. *Appl. Phys. Lett.* **87**, 023505 (2005).
12 Tu, C.-H., Lai, Y.-S. & Kwong, D.-L. Electrical switching and transport in the Si/organic monolayer/Au and Si/organic bilayer/Al devices. *Appl. Phys. Lett.* **89**, 062105 (2006).
13 Kolosov, D., English, D. S., Bulovic, V., Barbara, P. F., Forrest, S. R. & Thompson, M. E. Direct observation of structural changes in organic light emitting devices during degradation. *J. Appl. Phys.* **90**, 3242–3247 (2001).
14 Yang, Y., Ouyang, J., Ma, L., Tseng, R. H. & Chu, C. W. Electrical switching and bistability in organic/polymeric thin films and memory devices. *Adv. Funct. Mater.* **16**, 1001–1014 (2006).
15 Ling, Q. D., Liaw, D. J., Zhu, C., Chan, D. S. H., Kang, E. T. & Neoh, K. G. Polymer electronic memories: materials, devices and mechanisms. *Prog. Polym. Sci.* **33**, 917–978 (2008).
16 Kurosawa, T., Higashihara, T. & Ueda, M. Polyimide memory: a pithy guideline for future applications. *Polym. Chem.* **4**, 16 (2013).
17 Hahm, S. G., Ko, Y. G., Kwon, W. & Ree, M. Programmable digital polymer memories. *Curr. Opin. Chem. Eng.* **2**, 79–87 (2013).
18 Lin, W. P., Liu, S. J., Gong, T., Zhao, Q. & Huang, W. Polymer-based resistive memory materials and devices. *Adv. Mater.* **26**, 570–606 (2014).
19 Bandyopadhyay, A. & Pal, A. J. Multilevel conductivity and conductance switching in supramolecular structures of an organic molecule. *Appl. Phys. Lett.* **84**, 999–1001 (2004).
20 Ko, Y., Hahm, S. G., Murata, K., Kim, Y. Y., Ree, B. J., Song, S., Michinobu, T. & Ree, M. New fullerene-based polymers and their electrical memory characteristics. *Macromolecules* **47**, 8154–8163 (2014).
21 Scott, J. & Bozano, L. Nonvolatile memory elements based on organic materials. *Adv. Mater.* **19**, 1452–1463 (2007).
22 Henisch, H. K., Meyers, J. A., Callarotti, R. C. & Schmidt, P. E. Switching in organic polymer films. *Thin Solid Films* **51**, 265–274 (1978).
23 Ma, D., Aguiar, M., Freire, J. A. & Hümmelgen, I. A. Organic reversible switching devices for memory applications. *Adv. Mater.* **12**, 1063–1066 (2000).
24 Ling, Q., Song, Y., Ding, S. J., Zhu, C., Chan, D. S. H., Kwong, D.-L., Kang, E.-T. & Neoh, K.-G. Non-volatile polymer memory device based on a novel copolymer of *N*-vinylcarbazole and Eu-complexed vinylbenzoate. *Adv. Mater.* **17**, 455–459 (2005).
25 Lai, Y.-S., Tu, C.-H., Kwong, D.-L. & Chen, J. S. Bistable resistance switching of poly(N-vinylcarbazole) films for nonvolatile memory applications. *Appl. Phys. Lett.* **87**, 122101–122103 (2005).
26 Smits, J., Meskers, S. J., Janssen, R. & Marsman, A. & de Leeuw, D. Electrically rewritable memory cells from poly(3-hexylthiophene) schottky diodes. *Adv. Mater.* **17**, 1169–1173 (2005).
27 Baek, S., Lee, D., Kim, J., Hong, S. H., Kim, O. & Ree, M. Novel digital nonvolatile memory devices based on semiconducting polymer thin films. *Adv. Funct. Mater.* **17**, 2637–2644 (2007).
28 Kim, J., Cho, S., Choi, S., Baek, S., Lee, D., Kim, O., Park, S.-M. & Ree, M. Novel electrical properties of nanoscale thin films of a semiconducting polymer: quantitative current-sensing AFM analysis. *Langmuir* **23**, 9024–9030 (2007).
29 Hong, S.-H., Kim, O., Choi, S. & Ree, M. Bipolar resistive switching in a single layer memory device based on a conjugated copolymer. *Appl. Phys. Lett.* **91**, 093517 (2007).
30 Choi, S., Hong, S. H., Cho, S. H., Park, S., Park, S. M., Kim, O. & Ree, M. High-performance programmable memory devices based on hyperbranched copper phthalocyanine polymer thin films. *Adv. Mater.* **20**, 1766–1771 (2008).
31 Lee, J. S., Cho, J., Lee, C., Kim, I., Park, J., Kim, Y. M., Shin, H., Lee, J. & Caruso, F. Layer-by-layer assembled charge-trap memory devices with adjustable electronic properties. *Nat. Nanotechnol.* **2**, 790–795 (2007).
32 Ree, B. J., Kwon, W., Kim, K., Ko, Y., Kim, Y., Lee, H. & Ree, M. Clues to the electrical switching mechanism of carbazole-containing polyimide thin films. *ACS Appl. Mater. Interf.* **6**, 21692–21701 (2014).
33 Ko, Y., Kwon, W., Yen, H., Chang, C., Kim, D. M. & Kim, K. Various digital memory behaviors of functional aromatic polyimides based on electron donor and acceptor substituted triphenylamines. *Macromolecules* **45**, 3749–3758 (2012).
34 Mittal K. L. (ed.) *Polyimides and Other High Temperature Polymers: Synthesis, Characterization and Applications*, 2nd edn (VSP: Boston, USA, 2003).
35 Lee, S. G., Lim, S. H., Park, N. R., Choi, K. Y., Yi, M. H. & Shin, D. M. Surface effects on photo-alignment of polyimide blends containing cinnamoyl moiety. *Mol. Cryst. Liq. Cryst.* **507**, 283–289 (2009).
36 Chen, H. & Yin, J. I. E. Synthesis and characterization of negative-type photosensitive hyperbranched polyimides with excellent organosolubility from an A_2+B_3 monomer system. *J. Polym. Sci. Part A Polym. Chem. Ed.* **86**, 1735–1744 (2003).
37 Sasaki, A., Aoshima, H., Nagano, S. & Seki, T. A versatile photochemical procedure to introduce a photoreactive molecular layer onto a polyimide film for liquid crystal alignment. *Polym. J.* **44**, 639–645 (2012).
38 Ree, M., Nunes, T. L. & Chen, K. J. Structure and properties of a photosensitive polyimide: effect of photosensitive group". *J. Polym. Sci. Part B Polym. Phys. Ed.* **33**, 453–465 (1995).
39 Ree, M., Kim, S. I. & Lee, S. W. Alignment behavior of liquid-crystals on thin films of photosensitive polymers: effects of photoreactive group and UV-exposure". *Synth. Metals* **117**, 273–275 (2001).
40 Lee, S. W., Kim, S. I., Lee, B., Kim, H. C., Chang, T. & Ree, M. A soluble photoreactive polyimide bearing the coumarin chromophore in the side group: photoreaction, photoinduced molecular reorientation, and liquid-crystal alignability in thin films. *Langmuir* **19**, 10381–10389 (2003).
41 Chae, B., Lee, S. W., Ree, M., Jung, Y. M. & Kim, S. B. Photoreaction and molecular reorientation in a nanoscaled ilm of poly(methyl 4-(methacryloyloxy)cinnamate) studied by two-dimensional FTIR and UV correlation spectroscopy. *Langmuir* **19**, 687–695 (2003).
42 Lee, S. W., Kim, S. I., Lee, B., Choi, W., Chae, B., Kim, S. B. & Ree, M. Photoreactions and photoinduced molecular reorientations of nanoscale films of a photoreactive polyimide, and their alignment of liquid crystals. *Macromolecules* **36**, 6527–6536 (2003).
43 Hahm, S. G., Lee, T. J. & Ree, M. Photo- and rubbing-alignable brush-polyimides bearing three different chromophores. *Adv. Funct. Mater.* **17**, 1359–1370 (2007).
44 Hahm, S. G., Lee, S. W., Lee, T. J., Cho, S. A., Chae, B., Jung, Y. M., Kim, S. B. & Ree, M. UV-driven switching of chain orientation and liquid crystal alignment in

nanoscale thin films of a novel polyimide bearing stilbene moieties in the backbone. *J. Phys. Chem. B* **112**, 4900–4912 (2008).
45 Campbell, A. J., Bradley, D. D. C. & Lidzey, D. G. Space-charge limited conduction with traps in poly(phenylene vinylene) light emitting diodes. *J. Appl. Phys.* **82**, 6326–6342 (1997).
46 Jensen, K. L. Electron emission theory and its application: Folwer-Norheim equation beyond. *J. Vac. Sci. Technol. B* **21**, 1528–1544 (2003).
47 Frenkel, J. On pre-breakdown phenomena in insulators and electronic semi-conductors. *Phys. Rev.* **54**, 647–648 (1938).
48 Laurent, C., Kay, E. & Souag, N. Dielectric breakdown of polymer films containing metal clusters. *J. Appl. Phys.* **64**, 336–343 (1988).
49 Mark, P. & Helfrich, W. Space-sharge-limited currents in organic crystals. *J. Appl. Phys.* **33**, 205–215 (1962).

Supplementary Information accompanies the paper on the NPG Asia Materials website (http://www.nature.com/am)